arXiv:1602.08870v2 [cond-mat.soft] 1 May 2016

Free energy approach to micellization and aggregation: Equilibrium, metastability, and kinetics

Haim Diamant[a], David Andelman[b]

[a] *Raymond and Beverly Sackler School of Chemistry, Tel Aviv University, Tel Aviv 6997801, Israel*
[b] *Raymond and Beverly Sackler School of Physics & Astronomy, Tel Aviv University, Tel Aviv 6997801, Israel*

Abstract

We review a recently developed micellization theory, which is based on a free-energy approach and offers several advantages over the conventional one, based on mass action and rate equations. As all the results are derived from a single free-energy expression, one can adapt the theory to different scenarios by merely modifying the initial expression. We present results concerning various features of micellization out of equilibrium, such as the existence of metastable aggregates (premicelles), micellar nucleation and growth, transient aggregates, and final relaxation toward equilibrium. Several predictions that await experimental investigation are discussed.

1. Introduction

Micellization — the self-assembly of amphiphilic molecules into nano-scale aggregates in solution above a well-defined concentration (the CMC) — is a well-studied phenomenon [1–7]; arguably, the science of micelles predates nano-science by several decades. Theoretically, too, micellization is an old problem, dating back to the recognition of the hydrophobic effect [1, 8]. From the chemical-physics point of view, it can be viewed as a restricted demixing process [9], where the growth of the new phase is terminated at a finite characteristic size ("micro-phase separation").

The prevalent thermodynamic theory for micelles at equilibrium has been the one by Israelachvili, Mitchell, and Ninham [10]. It combines mass-action thermodynamic considerations with geometrical packing arguments, to account for the CMC and the aggregate shape and size. Various extensions to this theory, incorporating additional molecular details, were subsequently introduced (e.g., Ref. [11]).

Concerning the kinetics of aggregation, the prevalent approach can be traced back to Smoluchowski's classical theory of coagulation [12], which is based on a set of reaction-rate equations, the "reactants" being the various-sized aggregates. Its application to surfactant micellization, progressing through monomeric step-like growth/disintegration, is described by the Becker-Döring equations [13] — an infinite set of ordinary differential kinetic equations, which is written for the concentrations of aggregates, and whose linearization yields a discrete spectrum of relaxation rates [14]. This approach was criticized for its restriction to single-monomer kinetics, disregarding effects of micellar fusion and fission [15–17], and was argued to be limited to cases of high CMC and small aggregation number [16].

We begin the discussion with the basic ingredients common to any theory of micellization. In its simplest form, a surfactant solution is a binary mixture of surfactant and solvent. As such, it has three intensive control parameters, e.g., the temperature T, pressure p, and total volume fraction of surfactant Φ, or, alternatively, T, p, and the surfactant chemical potential μ. The choice of control parameters is immaterial if the solution is at thermal equilibrium. Its kinetics, however, can strongly depend on the specific constraints, e.g., whether the system is closed (fixed Φ) or open (fixed μ). Given the

Email addresses: hdiamant@tau.ac.il (Haim Diamant), andelman@post.tau.ac.il (David Andelman)
URL: http://www.tau.ac.il/∼hdiamant (Haim Diamant), http://www.tau.ac.il/∼andelman (David Andelman)

three control parameters, the system has as free variables the set of volume fractions of aggregates containing k solute molecules, $\{\Phi_k\}_{k=1,2,...}$. During the kinetics of micelle formation these variables are time-dependent. (In more complex situations they may also be space-dependent.) At equilibrium they attain the steady values $\{\Phi_k\} = \{\Phi_k^{\rm eq}\}$. Various theories may differ in the way these dynamic variables are derived. Once $\{\Phi_k\}$ are known (either at or out-of-equilibrium), one can obtain the full distribution of aggregate sizes.

The free-energy approach to micellization is centered on the free-energy density of the solution, F. Considering a closed system, $F = F(T, p, \Phi, \{\Phi_k\})$, subject to the constraint $\sum_k \Phi_k = \Phi$. (From now on the dependence on T and p will be omitted for brevity.) The equilibrium state, meta-stable states, kinetic barriers, and time evolution of aggregation are obtained, respectively, as the global minimum, local minima, maxima, and time-dependent trajectories, along the multi-variable landscape defined by F. Thus, apart from presenting an alternative description of micellization, the free-energy formalism provides additional information on such issues as the properties of metastable aggregates, nucleation barriers, and relaxation processes. The aim of this contribution is to present the essence and main findings of this approach, as published in Refs. [18–21]. Theories of similar spirit were presented in Ref. [22] for the thermodynamics of surfactant micelles, Ref. [23] for the thermodynamics of block copolymer micelles, and Ref. [24] for fluctuations, metastability, and kinetics close to the CMC.

2. Free energy landscape

The free-energy landscape as defined above, $F(\Phi, \{\Phi_k\})$, is in principle of infinite dimensions. The analysis is made tractable if we assume that, for each thermodynamic state of the solution, the distribution of aggregate size is either sharply unimodal, describing only monomers, or sharply bimodal, describing monomers and micelles of size m. Given the total surfactant volume fraction Φ, this leaves only two relevant variables, Φ_1 and m. The volume fractions of aggregates and solvent are given by $\Phi_m = \Phi - \Phi_1$ and $1 - \Phi$, respectively.

Two simple ingredients are used for the formulation of F. The first is the Flory-Huggins theory of solutions. The second is a single phenomenological function, $u(m)$, which incorporates the detailed properties of the specific surfactant molecule and accounts for the free-energy gain of transferring that molecule from the aqueous-solution environment into a micelle of size m. The only requirement for $u(m)$ is that it should have a single maximum at a certain value of m, to ensure the stability of finite aggregates (i.e., to terminate the growth of the demixed phase). See Refs. [18, 22] for a specific choice of $u(m)$ and its relation to the properties of the surfactant molecule. The resulting free-energy density is

$$F(\Phi, \Phi_1, m) = \frac{\Phi_1}{n} \ln \Phi_1 + \frac{\Phi_m}{nm}[\ln \Phi_m - mu(m)] + (1 - \Phi) \ln(1 - \Phi). \quad (1)$$

This function accounts for the entropy of mixing of the three species (solvent, monomer, micelle), and the amphiphilic nature of the surfactant (through the non-monotonous $u(m)$). We have simplified this equation (the only equation in this article) and the formulae to follow by expressing energies in terms of the thermal energy, $k_{\rm B}T$, and volumes in terms of the solvent molecular volume, a^3; the surfactant molecular volume is taken to be na^3. All the results presented below derive from Eq. (1) through simple mathematical procedures whose details are found in Refs. [18–21].

As the total surfactant volume fraction Φ is increased, the shape of the manifold defined by $F(\Phi_1, m)$ at fixed Φ changes, revealing various regimes of aggregation, to be described below, and as schematically shown in Fig. 1. The features seen in Fig. 1 (free-energy wells and barriers) are typically of order $\sim 1\ k_{\rm B}T$ per molecule, which amounts to tens of $k_{\rm B}T$ per aggregate [18–21]. In the present review, which is focused on unifying underlying mechanisms, we will not get into further numerical details concerning specific systems. In the following discussion the term "state" refers to the *entire* solution, not to the state of the surfactant molecules; thus, an "aggregated state" means a solution containing both monomers and aggregates, with a given partitioning between the two, Φ_1 and Φ_m, and with a given aggregate size, m.

For any value of Φ, F of Eq. (1) has a single minimum along the Φ_1 axis, at $\Phi_1^*(\Phi, m)$. However, as long as the surfactant volume fraction Φ is sufficiently low, $F(\Phi_1^*, m)$ is monotonously increasing with m (Fig. 1(a)), which implies a global minimum for a purely monomeric solution (with $m = 1$).

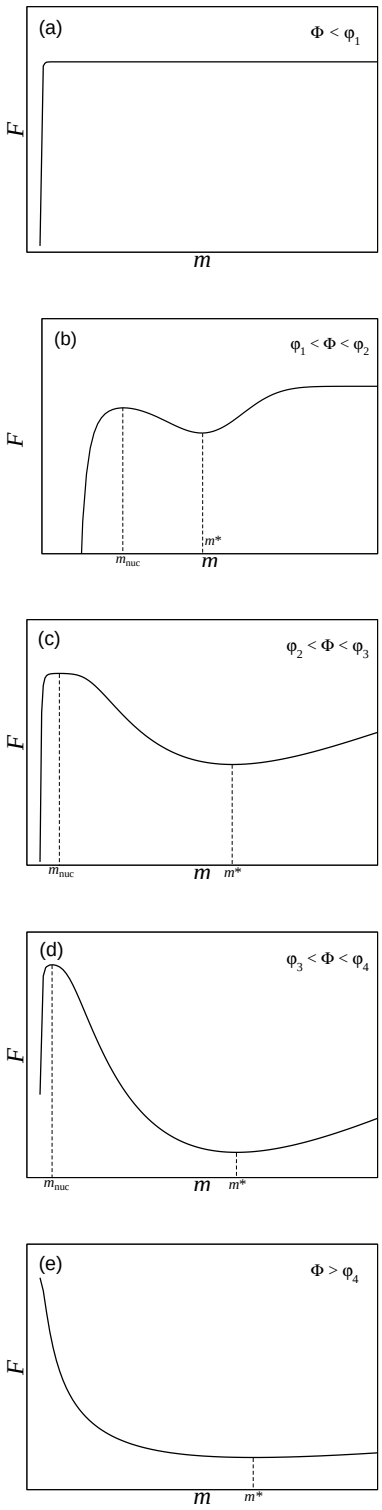

Figure 1: Schematic depiction of the free energy $F(\Phi_1^*(m), m)$ as a function of aggregation number m in the different concentration regimes, as obtained from Eq. (1).

3. Metastable premicelles and stable micelles

Above a certain volume fraction, $\Phi > \varphi_1$, $F(\Phi_1^*, m)$ becomes nonconvex as a function of m, and two extrema appear in addition to the minimum at the monomeric state (Fig. 1(b)). The first, which is a saddle point of $F(\Phi_1, m)$, represents an unstable state containing critical nuclei of size $m_{\rm nuc}$. The second, which is a local minimum of F, is a metastable state with aggregates of size m^*. In the analogy with first-order phase transitions, $\varphi_1(T, p)$ corresponds to the spinodal surface.

Although the metastable state appears as soon as $\Phi > \varphi_1$, closer inspection [18] reveals that only above a higher volume fraction, $\Phi > \varphi_2$ (Fig. 1(c)), does this state become significantly occupied. In the range $\varphi_1 < \Phi < \varphi_2$ the value of m^* increases, while the fraction of surfactant molecules in the metastable aggregated state remains negligible. For $\Phi > \varphi_2$, m^* remains almost constant, while the fraction of molecules in the metastable state increases.

Above a higher total volume fraction, $\Phi > \varphi_3$, the aggregated state (Φ_1^*, m^*) becomes the global free-energy minimum, and the purely monomeric state turns metastable (Fig. 1(d)). In the phase-transition analogy, $\varphi_3(T, p)$ is the binodal surface. The value $\Phi = \varphi_3$ corresponds to the critical micelle concentration (CMC) as it is commonly measured in experiments [18]. Thus, the range $\varphi_2 < \Phi < \varphi_3$ is identified as the *premicellar regime*, and the metastable aggregates are termed *premicelles*.

Finally, above a yet higher volume fraction, $\Phi > \varphi_4$, the purely monomeric state becomes unstable, and the aggregated state remains the sole free-energy minimum (Fig. 1(e)). In the phase-transition analogy $\varphi_4(T, p)$ represents the second spinodal surface of the mixture. We are not aware of an experiment in which this latter change in solution behavior was observed.

Returning to the issue of metastable aggregates, their appearance may be complicated by dynamic limitations. The results given above are obtained under the assumption that the solution has indefinite time to equilibrate. In practice there is a free-energy barrier, $F(\Phi_1^*, m_{\rm nuc})$, to cross, which may take too long and require the help of impurities to allow heterogeneous nucleation. Another dynamic issue is the lifetime of the metastable premicelles once they are formed. An analysis of the escape time from the free-energy minimum

$F(\Phi_1^*, m^*)$, across the barrier $F(\Phi_1^*, m_{\rm nuc})$, back to the monomeric state, has been performed based on Kramers' rate theory [20]. It showed that reasonably long (say, longer than seconds) premicellar lifetimes are obtained over a significant part of the premicellar ($\varphi_2 < \Phi < \varphi_3$) region. In addition, the polydispersity of premicelles was found to be only slightly larger than that of stable micelles [20].

Even after taking into account the limitations related to the occupancy and lifetime of the metastable state, the theory predicts a large extent of premicellar aggregation well below the CMC [20]. Indeed, any sharp transition is smoothed by finite-size effects, allowing the new state to be observed slightly below the transition point [25]. However, the predicted extent of premicellar aggregation can be an order of magnitude larger than what would be expected from a simple finite-size correction. The difference lies in the freedom to vary m as compared to a simple two-state case with monomers and aggregates of fixed m [18].

Over the years, and especially in the past decade, there have been quite a number of reports of premicelles, using a large variety of experimental techniques — steady-state and time-resolved fluorescence spectroscopy [26–34], fluorescence correlation spectroscopy (FCS) [35], UV absorption spectroscopy [36], dielectric relaxation spectroscopy [37], NMR [38], electrophoresis [39], and diffusion coefficient via radioactive labeling [40]. As an example, Fig. 2 shows results of FCS measurements in a cationic surfactant solution, revealing the formation of aggregates at concentrations three times smaller than the CMC [35]. Premicellar aggregation has been predicted also by another thermodynamic model [24], molecular dynamics simulations [41], as well as simulations of idealized systems [42]. Despite these numerous indications, the controversy surrounding premicellar aggregation has not been completely settled. (For alternative views, see Refs. [15, 17].) For example, since many observations rely on fluorescence techniques, one should consider the effect of the fluorescent dye on the micellization [43].

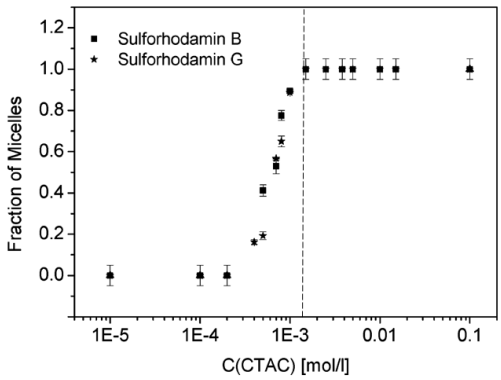

Figure 2: Results of FCS measurements in cationic surfactant (CTAC) solution. The data points show the fraction of anionic dye molecules (sulforhodamin B or G), associated with aggregates, as a function of surfactant concentration. As surfactant aggregates form, they bind the oppositely charged dye molecules, consequently appearing in the FCS measurement as a an additional, slowly diffusing, fluorescent species. The vertical dashed line indicates the CMC as found from conductivity measurements in CTAC solutions containing sulforhodamin G, precluding a possible reduction of the actual CMC by the dye. Adapted with permission from Zettl et al. [35]. Copyright (2005) American Chemical Society.

4. Kinetics of aggregation

The free-energy landscape, $F(\Phi_1, m)$, can be used also to study kinetic pathways of the surfactant solution toward equilibrium. These are derived as time-dependent trajectories on the surface (Φ_1, m), determined by certain constraints. The single additional input to the theory is a molecular time scale τ_0. Thus, different aggregation processes can be treated on the same footing. Another advantage of this approach is that, unlike models based on the Becker-Döring scheme, the kinetics is not limited to single-monomer steps.

The constraints that determine the trajectories become apparent if we assume that the time scales of different aggregation stages are well separated. Under this assumption, if we start from an out-of-equilibrium monomeric solution, we generally find a three-stage aggregation process, including slow nucleation, much faster growth, and ultimate relaxation toward equilibrium. The constrained trajectories depend also on the overall thermodynamic constraints imposed on the solution, e.g., whether it is a closed system (fixed Φ) or an open one (fixed μ), and may result in very different kinetic pathways. Below we outline the constrained paths which represent these stages, and the main results of this theory; full details, along with numerical examples, are found in Ref. [21].

Consider a closed system with total surfactant volume fraction above the CMC ($\Phi > \varphi_3$; Fig. 1(d)), starting from a purely monomeric state and ending at the equilibrium state $(\Phi_1^{\rm eq}, m^{\rm eq}) = (\Phi_1^*(m^*), m^*)$. The first stage is an increase of the

free energy from the metastable monomeric state to the saddle point $F(\Phi_1^*(m_{\rm nuc}), m_{\rm nuc})$, i.e., the formation of critical nuclei. Assuming that this slow activated process satisfies quasi-equilibrium constrains the trajectory to $(\Phi_1^*(m(t)), m(t))$, while $m(t)$ increases from 1 to $m_{\rm nuc}$. The total nucleation time is $\tau_{\rm nuc}(\Phi) = \tau_0 e^{\Delta F_{\rm nuc}}$, where $\Delta F_{\rm nuc} \sim F(\Phi_1^*(m_{\rm nuc}), m_{\rm nuc}) - F_1$ is the height of the barrier per nucleus (F_1 being the free energy of the monomeric state).

Various features of the nucleation stage can be calculated based on this description [21]. Taking the total surfactant volume fraction Φ further above the CMC leads to a sharp decrease in $\tau_{\rm nuc}$, a sharp increase in the concentration $c_{\rm nuc}$ of critical nuclei, and a gradual decrease in $m_{\rm nuc}$.

In contrast, the results for the nucleation in an open system are strikingly different. If transport of micelles from the bulk reservoir is blocked or negligible, the solution is in contact with the reservoir only through its monomeric concentration (the so-called inter-micellar concentration), which hardly changes with further increase of the bulk volume fraction above the CMC. Consequently, the critical nuclei remain relatively rare and large, and the nucleation barrier remains high. The resulting prediction is that homogeneous nucleation of micelles in an open system should be kinetically hindered.

The slow nucleation stage is followed by a much faster stage of aggregate growth. Assuming that the growth is fed exclusively by surrounding monomers implies that the number density of micelles, $(\Phi - \Phi_1)/(na^3 m)$, remains fixed and equal to $c_{\rm nuc}$. Thus, the appropriate constrained path representing this stage is $(\Phi_1(t) = \Phi - na^3 c_{\rm nuc} m(t), m(t))$. The rate of growth may be limited either by the diffusion of monomers to the aggregate or by the local kinetics at the aggregate. In the former case, the growth is proportional to the spatial gradient of Φ_1, whereas in the latter it is proportional to the thermodynamic driving force, i.e., the variation of F with m along the constrained path. Analysis shows that both mechanisms may be relevant in practice [21]. The growth stage ends at the minimum of F *along the constrained path* defined above. In general this point on the landscape does not coincide with the *global* minimum of F. Therefore, the transient aggregate size reached at the end of the growth stage, $\bar{m}$, may be either smaller or larger than the equilibrium size m^*.

In the last stage of growth, the closed solution relaxes toward the equilibrium state, $(\Phi_1^{\rm eq}, m^{\rm eq}) = (\Phi_1^*(m^*), m^*)$. Over this longer relaxation the constraint on the number of micelles is lifted. At the same time, nucleation or disintegration of entire micelles take too long. This implies that the evolution of this final stage should occur through micellar fusion (if $\bar{m} < m^*$) or fission (if $\bar{m} > m^*$). The relaxation rate is related again to the thermodynamic driving force; yet, in the latter stage it is given by the slope of F along the $[\phi_1^*(m(t)), m(t)]$ path toward equilibrium, without a constraint on the concentration of micelles. In this final relaxation stage the kinetics of an open system is again found to be strongly hindered.

Several kinetic characteristics described in this section have been supported by experiments and other theories. Time-resolved small angle x-ray scattering revealed the three stages presented above in block-copolymer micellization [44]. Three separate stages were obtained also by another model based on kinetic equations [45]. The possibility of transient micelles relaxing into micelles of different size was indicated by two other micellization models [9, 16], as well as idealized (two-dimensional) Monte-Carlo simulations [42]. The kinetic hindrance of micelle formation in open surfactant solutions is supported by dialysis experiments, where the diffusive contact with the reservoir does not allow the passage of micelles. The appearance of micelles on the monomeric side was found to take hours [46].

5. Concluding remarks

This short review has outlined the free-energy theoretical framework that was recently developed for micellization. The formulation is sufficiently general, in fact, to apply just as well to any finite-size aggregation in solution, e.g., the formation of surface-stabilized nanocrystals. This approach has several advantages, such as its consistent and self-contained account of different phenomena (all the results stemming from one free-energy function); its simplicity, which allows to obtain many of the results analytically and the rest by very basic numerics; and its easy extension to other scenarios (by modifying that single function). On the other hand, it should be kept in mind that the theory provides only a crude deterministic description of much more complicated stochastic phenomena. In particular, the assumption of a sharply bimodal distribution of aggregate sizes should be relaxed to obtain a re-

liable quantitative account of stages that involve crossing a nucleation barrier.

We would like to highlight a few experimental implications. The existence of metastable premicelles well below the CMC, as implied by the theory, has received significant experimental support (see Sec. 3), but is not considered as settled. Our present point of view is that intrinsic homogeneous nucleation of premicelles is kinetically suppressed and probably negligible. Their observation requires, therefore, heterogeneous nucleation facilitated by impurities [19]. Indeed, this sensitivity of premicellar nucleation is a possible explanation for conflicting experimental results. The potential appearance of transient micelles larger than their equilibrium size is another strong prediction, shared by other theories [9, 16], which to our knowledge has not been checked experimentally. Another prediction, which calls for more controlled experiments, is the very long kinetic suppression of micelle nucleation in open systems whose exchange with the reservoir is limited to monomers.

Finally, an interesting and unexplored aspect of micellization is the dynamics following a deep quench beyond the "spinodal" φ_4 (see Fig. 1(e)). Comparison to the well-studied spinodal decomposition of ordinary mixtures might underline the similarity and difference between micellization and demixing phase transitions.

Acknowledgments

We thank Martin Lenz for a helpful discussion. DA acknowledges support from the ISF-NSFC joint research program (Grant No. 885/15), the Israel Science Foundation (ISF) (Grant No. 438/12), and the United States–Israel Binational Science Foundation (BSF) (Grant No. 2012/060).

References

[1] C. Tanford, *The Hydrophobic Effect: Formation of Micelles and Biological Membranes*, Wiley, 1973.

[2] K. L. Mittal, *Micellization, Solubilization, and Microemulsions*, Vol. 1, Plenum Press, 1977.

[3] B. Lindman, B., H. Wennerstrom, *Micelles*, Springer-Verlag, 1980.

[4] J. N. Israelachvili, *Intermolecular and Surface Forces*, 2nd ed., Academic Press, 1992.

[5] *Micelles, Membranes, Microemulsions, and Monolayers*, W. M. Gelbart, A. Ben-Shaul, D. Roux (eds.), Springer, 1994.

[6] M. J. Rosen, *Surfactants and Interfacial Phenomena*, Wiley, 2004.

[7] R. Zana, *Dynamics of Surfactant Self-Assemblies*, CRC Press, 2005.

[8] W. Kauzmann, Adv. Protein Chem. **14**, 1-63 (1959).

[9] * N. A. M. Besseling, M. A. Cohen-Stuart, J. Chem. Phys. **110**, 5432-5436 (1999).

[10] * J. Israelachvili, J. Mitchell, B. W. Ninham, J. Chem. Soc. Faraday Trans. **72**, 1525-1568 (1976).

[11] R. Nagarajan, E. Ruckenstein, Langmuir **7**, 2934-2969 (1991).

[12] M. V. Smoluchowski, Physik. Z. **17**, 557-585 (1916).

[13] * R. Becker, W. Döring, Ann. Phys. **24**, 719-752 (1935).

[14] I. Babintsev, L. Adzhemyan, A. Shchekin, Alexander, J. Chem. Phys. **137**, 044902 (2012).

[15] W. Al-Soufi, L. Pineiro, M. Novo, J. Colloid Interface Sci. **370**, 102-110 (2012).

[16] * I. M. Griffiths, C. J. W. Breward, D. M. Colegate, P. J. Dellar, P. D. Howell, C. D. Bain, Soft Matter **9**, 853-863 (2013).

[17] L. Pineiro, M. Novo, W. Al-Soufi, Adv. Colloid Interface Sci. **215**, 1-12 (2015).

[18] R. Hadgiivanova, H. Diamant, J. Phys. Chem. B **111**, 8854-8859 (2007).

[19] R. Hadgiivanova, H. Diamant, J. Phys. Chem. B **114**, 7131 (2010).

[20] R. Hadgiivanova, H. Diamant, J. Chem. Phys. **130**, 114901 (2009).

[21] R. Hadgiivanova, H. Diamant, D. Andelman, J. Phys. Chem. B **115** 7268-7280 (2011).

[22] * L. Maibaum, A. R. Dinner, D. Chandler, J. Phys. Chem. B **108**, 6778-6781 (2004).

[23] I. A. Nyrkova, A. N. Semenov, Macromol. Theory Simul. **14**, 569-585 (2005).

[24] J. K. Bhattacharjee, U. Kaatze, J. Phys. Chem. B **117**, 3790-3797 (2013).

[25] T. L. Hill, *Thermodynamics of Small Systems*, Dover, 1994.

[26] S. Niu, K. R. Gopidas, N. J. Turro, G. Gabor, Langmuir **8**, 1271-1277 (1992).

[27] L. Sahoo, J. Sarangi, P. K. Misra, Bull. Chem. Soc. Jpn. **75**, 859-865 (2002).

[28] S. S. Jaffer, M. Sowmiya, S. K. Saha, P. Purkayastha, J. Colloid Interface Sci. **325**, 236-242 (2008).

[29] R. Barnadas-Rodriguez, J. Estelrich, J. Phys. Chem. B **113**, 1972-1982 (2009).

[30] M. Beija, A. Fedorov, M. T. Charreyre, J. M. G. Marinho, M. G. Jose, J. Phys. Chem. B **114**, 9977-9986 (2010).

[31] T. Sakai, Y. Kaneko, K. Tsujii, Langmuir **22**, 2039-2044 (2006).

[32] S. D. Choudhury, A. C. Bhasikuttan, H. Pal, J. Mohanty, Langmuir **27**, 12312-12321 (2011).

[33] M. Sowmiya, A. K. Tiwari, S. K. Saha, J. Colloid Iinterface Sci. **344**, 97-104 (2010).

[34] A. K. Tiwari, Sonu, M. Sowmiya, S. K. Saha,. J. Photochem. Photobiol. A Chem. **223**, 6-13 (2011).

[35] * H. Zettl, Y. Portnoy, M. Gottlieb, G. Krausch, J. Phys. Chem. B **109**, 13397-13401 (2005).

[36] J. Fu, Z. Cai, Y. Gong, S. E. O'Reilly, X. Hao, D. Zhao, Colloids Surfaces A **484**, 1-8 (2015).

[37] Z. Chen, X.-W. Li, K.-S. Zhao, J.-X. Xiao, L.-K. Yang, J. Phys. Chem. B **115**, 5766-5774 (2011).

[38] X. Cui, S. Mao, M. Liu, H. Yuan, Y. Du, Langmuir **24**, 10771-10775 (2008).

[39] R. Sabate, M. Gallardo, J. Estelrich, Electrophoresis **21**, 481-485 (2000).

[40] B. Lindman, B. Brun, J. Colloid Interface Sci. **42**, 388-399 (1973).

[41] D. N. LeBard, B. G. Levine, R. DeVane, W. Shinoda, M. L. Klein, Chem. Phys. Lett. **522**, 38-42 (2012).
[42] J. N. B. de Moraes, W. Figueiredo, Phys. Rev. E **87**, 062315 (2013).
[43] S. Freire, J. Bordello, D. Granadero, W. Al-Soufi, M. Novo, Photochem. Photobiol. Sci. **9**, 687-696 (2010).
[44] * R. Lund, L. Willner, D. Richter, Adv. Polymer Sci. **259**, 51-158 (2013).
[45] J. C. Neu, J. A. Cañizo, L. L. Bonilla, Phys. Rev. E **66**, 061406 (2002).
[46] Morigaki, K.; Walde, P.; Misran, M.; Robinson, B. H. Colloids Surfaces A **213** 37-44 (2003).